Journal of the European Ceramic Society 38 (2018) 4283–4289

Contents lists available at ScienceDirect

Journal of the European Ceramic Society

journal homepage: www.elsevier.com/locate/jeurceramsoc

Original Article

Surface tension-pressure superposition principle for anisotropic shrinkage of an ellipsoidal pore in viscous sintering

Shun Kanchika, Fumihiro Wakai*

Laboratory for Materials and Structures, Institute of Innovative Research, Tokyo Institute of Technology, R3-23 4259 Nagatsuta, Midori, Yokohama, 226-8503, Japan

ARTICLE INFO

Keywords:
Sintering
Simulation
Micromechanical modeling

ABSTRACT

The shrinkage of a spherical pore is a classical model of the final stage of sintering; however, closed pores observed in real sintering have irregular shapes, which can be approximated as ellipsoids in many cases. In this study, we used the finite element simulation to evaluate the anisotropic shrinkage of a non-spherical pore. The shape evolution was expressed as the superposition of the deformation of a pore driven by surface tension and the deformation of a void driven by remote pressure in the absence of surface tension. By using this superposition principle, we can predict the shape evolution of any spheroidal pore, which is affected by the initial aspect ratio, the remote pressure, and the gas pressure inside the pore. We analyzed the role of sintering stress tensor on the anisotropic shrinkage also.

1. Introduction

The shrinkage of a single spherical pore is the best microscopic model (Mackenzie-Shuttleworth model [1]) for understanding the final stage of viscous sintering, which occurs by viscous flow driven by surface tension and applied pressure. When the closed pore contains gases, the shrinkage rate of pore volume V_{pore} is expressed as:

$$\frac{1}{V_{pore}}\frac{dV_{pore}}{dt} = -\frac{3(\sigma^s + P_a - p_{pore})}{4\mu} \quad (1)$$

where μ is the viscosity, P_a is the uniform remote pressure, p_{pore} is the gas pressure inside the pore, and σ^s is the local sintering stress. The local sintering stress of a spherical pore is proportional to the surface energy γ_s and inversely proportional to the pore radius r ($\sigma^s = 2\gamma_s/r$). It is equal to the gas pressure, which is necessary to stop shrinkage under zero applied pressure. The densification is enhanced by the application of pressure, for example, in sinter forging, hot pressing, hot isostatic pressing [2], and spark plasma sintering.

The microstructural evolution in real sintering process of glass particles has been directly observed by using X-ray microtomography recently [3–8]. It has revealed how closed pores are formed by pinch-off, or break-up of pore channels [9]. In general, the formed pores are not perfect spheres, but have irregular shapes, which can be roughly approximated as ellipsoids in many cases.

The deformation of an ellipsoidal inclusion can be analyzed by using Eshelby's method [10,11] for the problem of elasticity. This method was extended to viscous flow by Bilby, Eshelby, and Kundu [12]. The first attempt to analyze the shrinkage of an ellipsoidal pore was made by Olevsky and Skorohod [13] using Eshelby's approach. For an elliptical pore in two dimensions, Hopper [14] reported the pore shrank with a constant axial ratio. On the other hand, Van de Vorst [15] found that an elliptical pore became more anisotropic as it shrank. Tanveer and Vasconcelos [16] predicted that an elliptical pore shrank to a slit. Pozrikidis [17] showed the eccentricity of an elliptical pore increased monotonically in time. Crowdy [18] found that initially circular pores, which were arranged in a row, became ellipse-like in shape under evolution. Olevsky [19] pointed out that the anisotropy of both sintering stress and viscosity were factors necessary to describe the anisotropic shrinkage of porous materials containing ellipsoidal pores aligned in a specific direction. Wakai [20] proposed a deformation model of a non-spherical pore as the sum of the anisotropic shrinkage driven by the hydrostatic component of sintering stress and the spheroidization driven by the deviatoric component by using the Eshelby's solution. However, the classical Eshelby formalism must be modified when the surface tension cannot be neglected in nanostructured materials [21,22]. Especially, the ellipsoidal pore deforms non-uniformly under the action of surface tension.

In order to understand the evolution of pore shape in the final stage, we simulate the anisotropic shrinkage of non-spherical pores as a response to the sintering stress, the remote pressure, and the gas pressure inside the pore by using the finite element method (FEM). Three typical cases are considered here: (1) Void ($P_a \gg \sigma^s$, $p_{pore} = 0$), (2) Pore ($\sigma^s > 0$, $P_a = 0$, $p_{pore} = 0$), and (3) Bubble ($\sigma^s > 0$, $P_a = 0$, V_{pore}=

* Corresponding author.
E-mail address: wakai.f.aa@m.titech.ac.jp (F. Wakai).

https://doi.org/10.1016/j.jeurceramsoc.2018.05.015
Received 19 March 2018; Received in revised form 9 May 2018; Accepted 12 May 2018

constant). A very large pore is considered as a void deforming under remote pressure, since the effect of surface tension is ignored (case 1). As the pore size decreases to micro- and nano-scales, the surface tension on the pore surface becomes very large. In this case (case 2), the pore shrinkage is driven by the sintering stress. When there is an insoluble gas inside the closed pore, the gas pressure increases with decreasing the pore volume. The shrinkage stops when the gas pressure balances with the sintering stress. The pore is considered as a bubble in this case (case 3). The non-spherical bubble becomes more spherical, i.e. the spheroidization occurs, while keeping its volume constant. If the gas is soluble to the glass and in equilibrium, the pore keeps shrinking by the driving force $\sigma^s - p_{pore} > 0$, where p_{pore} maintains a constant value. Spherical pores, frequently observed in experiments, are the result of residual gas pressure inside the closed pore, which is trapped during sintering in atmospheres, or evolved from the glass in vacuum sintering [1]. When there is no gas inside the closed pore, the non-spherical pore becomes more anisotropic as it shrinks under the surface tension. We will show how anisotropic shrinkage of a pore depends on the gas pressure inside, the applied pressure, and the sintering stress. We found a superposition principle, so that the anisotropic shrinkage at any pressure and at any gas pressure could be predicted from the results of case 1 (Void) and case 2 (pore) only. Our analysis will be a basis for understanding the micromechanics behind the macroscopic shrinkage. Especially, it will be useful when we can obtain the detailed knowledge of microstructural evolution from the real-time observation using synchrotron X-ray microtomography [23].

2. Simulation method

Consider an axisymmetric ellipsoidal pore (spheroid) which has semi-axes $a = b$, c as shown in Fig. 1. The radius of the equivalent sphere is $r = (a^2c)^{1/3}$. The pore is centered at the origin inside an incompressible viscous fluid with a viscosity μ. The boundary of the viscous fluid is a concentric sphere with radius $7r$. The viscous flow is described by Stokes equation:

$$\frac{\partial p}{\partial x_i} = \mu \frac{\partial^2 u_i}{\partial x_j \partial x_j} \tag{2}$$

where u_i is the velocity, and p is the pressure. The mass conservation is expressed as:

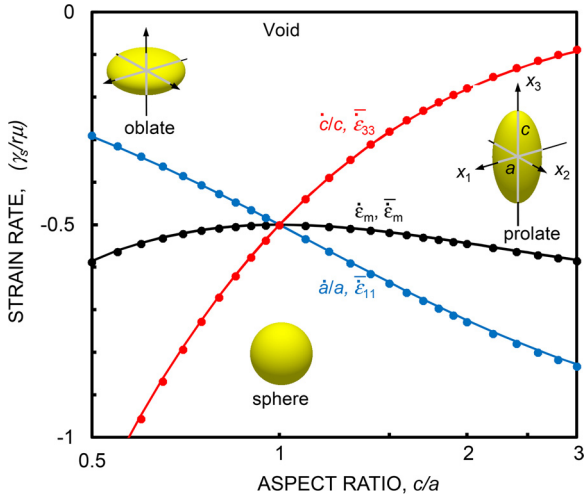

Fig. 1. Shrinkage of a spheroidal void under applied pressure $P_a = 2\gamma_s/r$. Circles show the axial strain rates $\dot{a}/a$ and $\dot{c}/c$ obtained by FEM simulation. Solid line shows Budiansky's result. The average strain rate, $\bar{\dot{\varepsilon}}_{11}$ and $\bar{\dot{\varepsilon}}_{33}$, calculated by Eq. (6) agrees with axial strain rates. The ellipsoidal void deforms affinely in accordance with Eshelby's analysis.

$$\frac{\partial u_i}{\partial x_i} = 0 \tag{3}$$

The summation convention for repeated indices is applied throughout this paper.

The shape evolution of the spheroidal pore was simulated by using the finite element package ANSYS, Polyflow (Ver. 14.5). We used an axisymmetric model about the x_3 -axis and symmetric about the $x_1 - x_2$ plane, so that one fourth of the pore is modeled. For the case 1 (Void), the normal traction equal to $P_a = 2\gamma_s/r$ was imposed on the outer boundary of the viscous fluid. The normal traction was zero on the pore surface. For the case 2 (Pore) and the case 3 (Bubble), the normal traction is imposed on the pore surface assuming an isotropic surface energy:

$$\sigma_n = \gamma_s \kappa \tag{4}$$

where κ is the curvature, which depends on position. The normal traction on the outer boundary was set to zero. For case 3 (Bubble), the pore space was filled with an inviscid incompressible fluid. For the numerical calculation, we used $\mu' = 1 \times 10^{-5}\mu$ for its viscosity. The effect of gravity was not considered in the present simulation.

The simulations were conducted for spheroids with given aspect ratios c/a. The dimensionless time is defined as:

$$t^* = \gamma_s t / r_0 \mu \tag{5}$$

where r_0 is the initial radius of the equivalent sphere. We calculated the axial strain rates ($\dot{a}/a$, $\dot{c}/c$) and the average strain rates ($\bar{\dot{\varepsilon}}_{11}$, $\bar{\dot{\varepsilon}}_{33}$) for the given aspect ratio at the dimensionless time $t^* = 5 \times 10^{-3}$ for case 1 (Void), case 2 (Pore), and case 3 (Bubble). The average strain rates were calculated from the surface integral by using the divergence theorem of Gauss:

$$\bar{\dot{\varepsilon}}_{ij} \equiv \frac{1}{2V_{pore}} \int_{V_{pore}} \left(\frac{\partial u_i}{\partial x_j} + \frac{\partial u_j}{\partial x_i} \right) dV = \frac{1}{2V_{pore}} \int_{S_{pore}} (u_i n_j + u_j n_i) dA \tag{6}$$

We also performed the finite element simulation of the spheroidization, or rounding, of an ellipsoidal particle, for the comparison with the spheroidization of a pore.

3. Results

3.1. Anisotropic shrinkage of a void (case 1)

The axial strain rates ($\dot{a}/a$ and $\dot{c}/c$) of a spheroidal void under remote pressure $P_a = 2\gamma_s/r$ are plotted as a function of aspect ratio in Fig. 1. Filled circles show the simulation results of axial strain rates. The apparent shrinkage rate is calculated from the axial strain rates $\dot{\varepsilon}_m = (2\dot{a}/a + \dot{c}/c)/3$. The shrinkage of the void is isotropic for a sphere ($\dot{c}/c = \dot{a}/a$ at $c/a = 1$), but anisotropic for oblate voids ($\dot{c}/c < \dot{a}/a$ for $c/a < 1$) and prolate voids ($\dot{c}/c > \dot{a}/a$ for $c/a > 1$). The spheroidal void becomes more anisotropic as it shrinks under the applied pressure. Solid lines show the theoretical prediction of axial strain rates by Budiansky, Hutchinson, and Slutsky [24]. They applied Eshelby's analysis to the collapse of an isolated void in a viscous materials. The present simulation results agreed with their theoretical prediction exactly. The axial strain rates at $P_a = 2\gamma_s/r$ are approximated as functions of aspect ratio $\lambda = c/a$ in the range $0.5 \le \lambda \le 3$:

$$(\dot{a}/a)_{void} = -0.0256\lambda^3 - 0.2134\lambda^2 - 0.6871\lambda \, (\gamma_s/r\mu) \tag{7}$$

$$(\dot{c}/c)_{void} = (\dot{a}/a)_{void}/\lambda^2 \, (\gamma_s/r\mu) \tag{8}$$

The average strain rates ($\bar{\dot{\varepsilon}}_{11}$, $\bar{\dot{\varepsilon}}_{33}$, $\bar{\dot{\varepsilon}}_m = (2\bar{\dot{\varepsilon}}_{11} + \bar{\dot{\varepsilon}}_{33})/3$) defined by Eq. (6) agreed with the axial strain rates in the present simulation ($\bar{\dot{\varepsilon}}_{11} = \dot{a}/a$, $\bar{\dot{\varepsilon}}_{33} = \dot{c}/c$, $\bar{\dot{\varepsilon}}_m = \dot{\varepsilon}_m$). This results show that the surface motion of spheroidal void is an affine deformation ($u_i = \dot{\varepsilon}_{ij} x_j$) in accordance with Eshelby's analysis.